

We are IntechOpen, the world's leading publisher of Open Access books Built by scientists, for scientists

6,900

Open access books available

186,000

International authors and editors

200M

Downloads

Our authors are among the

154

Countries delivered to

TOP 1%

most cited scientists

12.2%

Contributors from top 500 universities



WEB OF SCIENCE™

Selection of our books indexed in the Book Citation Index
in Web of Science™ Core Collection (BKCI)

Interested in publishing with us?
Contact book.department@intechopen.com

Numbers displayed above are based on latest data collected.
For more information visit www.intechopen.com



Electrochemical Studies of Corrosion in Liquid Electrolytes for Energy Conversion Applications at Elevated Temperatures

Aleksey V. Nikiforov, Irina M. Petrushina and
Niels J. Bjerrum

Additional information is available at the end of the chapter

<http://dx.doi.org/10.5772/64003>

Abstract

Stainless steels (AISI 316, 321 and 347), high-nickel alloys (Hasteloy®C-276 and Inconel®625), tantalum, nickel, titanium, tungsten, molybdenum, niobium, platinum, and gold were tested for corrosion resistance in molten KH_2PO_4 (or $\text{KH}_2\text{PO}_4\text{-K}_2\text{H}_2\text{P}_2\text{O}_7$) as a promising electrolyte for the intermediate-temperature (200–400°C) water electrolysis. Pt, Ta, Nb, Ti, Inconel®625, and Ni demonstrated high corrosion resistance. Au and the rest of the tested materials were not corrosion resistant. It means that Ni, Ti and Inconel®625 may be used as relatively cheap construction materials for the intermediate-temperature water electrolyzer.

Keywords: Intermediate-temperature electrolysis, bipolar plates, nickel stability, corrosion, oxygen evolution, molten salts

1. Introduction

Use of the renewable energy is often combined with storage of excess energy. Water electrolysis is one of the most effective ways of energy storage. Produced hydrogen can be used in the hydrogen refueling stations for fuel cell cars or used as a reactant with CO_2 in the Sabatier synthesis producing methane.

There are two types of the available commercial electrolyzers with different electrolyte: (1) alkaline water electrolyzer (AWE) (2) proton exchange membrane (PEM) water electrolyzer.

The latter has much higher voltage efficiency than the former system. However, in alkaline electrolyzers, non-noble Ni-based catalysts are used, but in the PEM water electrolyzers, the noble Pt and IrO₂ catalysts are used. The use of noble metal catalysts could become a problem for mass production.

Intermediate temperature water electrolysis has a potential to combine high efficiency with cheap catalysts. The molten KH₂PO₄ is a promising candidate for a proton-conducting electrolyte. Moreover, it has been shown that WC is a better catalyst than Pt for the hydrogen evolution reaction in this electrolyte at 260°C [1].

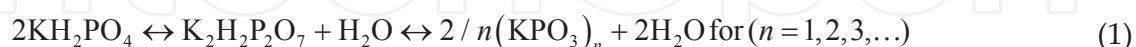
In this paper, corrosion resistance of stainless steels (AISI 316, 321 and 347), high-nickel alloys (Hasteloy®C-276, Inconel®625), tantalum, nickel, titanium, tungsten, molybdenum, niobium, platinum, and gold was studied in the molten KH₂PO₄-K₂H₂P₂O₇ system.

Earlier, we have studied corrosion behavior of the same materials at 150°C in concentrated phosphoric acid as model system for the polybenzimidazol/phosphoric acid electrolyte [2–4]. This polymeric electrolyte was studied as a high-temperature (up to 200°C) alternative to the Nafion® electrolyte in PEM water electrolyzers. Unfortunately, the only material which was corrosion stable under these conditions was tantalum. It would be logic to expect similar results at 200°C in KH₂PO₄.

Electrochemical behavior of Pt and Au was already studied in the potassium dihydrogen sulfate melt in argon atmosphere at 265°C. It was found that the electrochemical stability window for the Pt electrode was 1.05 V with the hydrogen evolution reaction as the cathodic limit and the oxygen evolution reaction as the anodic limit. It has been also shown that gold is corrosion unstable at positive polarization.

Recently, we have studied the thermal behavior of molten potassium dihydrogen phosphate using differential scanning calorimetry and Raman spectroscopy [5].

It has been shown if the vessel is not pressurized at temperatures higher than ~100°C water tends to evaporate. KH₂PO₄ salts have various applications [6] and recently also the application of the melt as an electrolyte for high temperature water electrolysis was suggested [7]. Upon the melting process, water molecules are considered to participate in the formation of eutectic mixtures among phosphates and other salts, due to reactions such as [8, 9]:



where the melt loses water by evaporation, starting at ~180°C [10].

Further heating of the system under open atmosphere will inevitably decompose it to the metaphosphate salt (KPO₃)_n and water vapor. The KH₂PO₄ melt binds water via hydrogen bonds [6] and is a proton-conducting electrolyte [4, 6]. In the present work, we therefore tried applying it for water electrolysis since preliminary studies in this connection have shown promising results for the conductivity of several molten KH₂PO₄ salt mixtures containing more or less water and under their own water vapor pressure at 240–320°C temperature range in

the [6]. It was shown that the KH_2PO_4 melts have conductivities in the order of $\sim 0.30 \text{ S cm}^{-1}$ at $\sim 300^\circ\text{C}$ and thus constitute promising electrolytes for pressurized water electrolysis at elevated temperatures. The melting point of the KH_2PO_4 electrolyte under its own vapor pressure was determined to be 272°C [6], although lower melting point values around $\sim 253^\circ\text{C}$ often have been reported in the literature [4, 11].

There is evidently no true melting point at atmospheric pressure, as fusion is simultaneously accompanied by decomposition due to loss of water, as shown by evolution of gas (water vapor) from the crystals [12].

Transfer from KH_2PO_4 to $(\text{KPO}_3)_n$ leads to solidification of the molten salt and therefore makes the electrochemical measurements impossible. Because of the temperature of our experiment and the atmospheric pressure, it is natural to assume that in the present study the electrolyte was molten mixture of KH_2PO_4 and $\text{K}_2\text{H}_2\text{P}_2\text{O}_7$.

2. Experimental

2.1. Materials

The chemicals KH_2PO_4 , KHSO_4 (Sigma-Aldrich, p.a.), and Ag_2SO_4 (Heraeus, 99.9% pure) were used as received.

2.2. Electrode preparation

The gold and platinum wires sealed in Pyrex tubes served as working electrodes (the diameter of the wires was 0.2 and 0.4 mm, respectively). The other metal wires were sealed in alumina tubes with outer and inner diameter 4 and 2 mm, respectively. CC180W coating paste was used for sealing the wires inside the tubes and was provided by CeProTec (Germany). CVD tantalum-coated stainless steel AISI 316L (diameter 1.0 mm) was provided by Tantaline A/S (Denmark). Nickel and niobium wires (diameter 1.0 mm) were provided by Good Fellow Cambridge Limited (England). Both the nickel wire with a purity of 99.98% and hard tempered the niobium wire with a purity of 99.9% were annealed. W, Mo, Ti, and Ta wires with diameter 1 mm were provided by ChemPur GmbH, Germany. The rest of the metal wires were provided by Sigma Aerospace Metals LLC. Depending on the composition of the wires, the diameter varied from 0.5 to 0.7 mm. The working electrode area among all tested materials varied from 0.08 to 0.72 cm^2 . A platinum wire spiral served as a counter electrode. The reference electrode was a silver wire placed in a Pyrex cylindrical chamber with a Pyrex grade "3" frit bottom. A melt of KHSO_4 saturated with Ag_2SO_4 was used as an electrolyte for the reference electrode. This electrode proved to be reliable during our previous studies [12, 13]. The potential difference between the $\text{Ag}/\text{Ag}_2\text{SO}_4$ and the normal hydrogen electrode (NHE) is approximately 0.7 V at room temperature [14]. Typical chemical compositions of stainless steels and nickel-based alloys investigated in this work are given in **Table 1**.

Alloy type	Ni	Co	Cr	Mo	W	Fe	Si	Mn	C	Al	Ti	Other	Nb + Ta
AISI 347	9.0– 13.0	–	17–19	–	–	Bal.	1.0	2.0	0.08	–	–	–	0.8
AISI 321	9.0– 12.0	–	17–19	–	–	Bal.	1.0	2.0	0.08	–	0.4– 0.7	–	–
AISI 316L	10.0– 13.0	–	16.5– 18.5	2.0–2.5	–	Bal.	1.0	2.0	0.03	–	–	N less 0.11	–
Hastelloy®C-276	57	2.5	15.5	16.0	3.75	5.5	0.08	1.0	0.02	–	–	V 0.35	–
Inconel®625	62	1.0	21.5	9.0	–	5.0	0.5	0.5	0.1	0.4	0.4	–	3.5

Table 1. Alloy chemical composition.

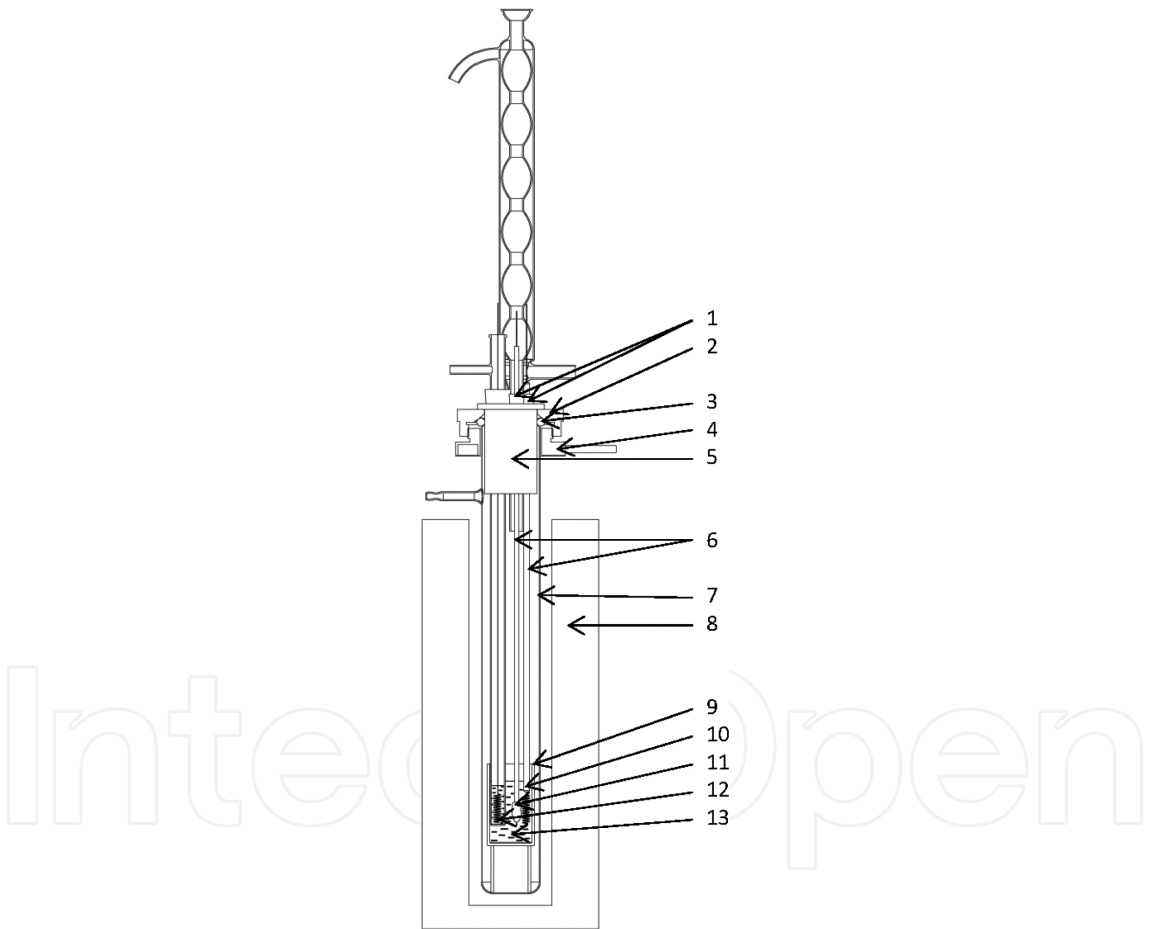


Figure 1. The electrochemical cell: (1) silicon rubber stoppers; (2) stainless steel cover; (3) viton ring; (4) stainless steel lid; (5) teflon lid; (6) ceramic tubes; (7) quartz tube; (8) oven; (9) pyrex glass; (10) counter electrode; (11) working electrode; (12) reference electrode; and (13) electrolyte.

Voltammetric measurements were performed in a three-electrode quartz cell shown in **Figure 1**. The cell was placed in a vertical aluminum-bronze alloy block furnace with temperature regulation within $\pm 1^{\circ}\text{C}$. The temperature inside the cell was measured by a chromel-alumel

thermocouple in a stainless steel cover. The thermocouple was placed between the walls of the Pyrex glass (position 9 in **Figure 1**) and the quartz tube (position 7 in **Figure 1**).

A condenser was placed above the electrochemical cell so that the escaping water from the melt could be condensed and run back into the melt. Because the amount of water which still escapes from heated KH_2PO_4 is not known, the composition of the melt is given as $\text{KH}_2\text{PO}_4/\text{K}_2\text{H}_2\text{P}_2\text{O}_7$.

All steady-state voltammetric tests were performed at 260°C in air using potentiostat model VersaSTAT 3 and VersaStudio software by Princeton Applied research. For each experiment, polarization was initiated at -1 V vs. $\text{Ag}/\text{Ag}_2\text{SO}_4$ reference electrode, followed to 1.4 V and then the polarization direction was reversed to the negative direction back to -1 V . The exchange current densities obtained during the backward scan were used to evaluate corrosion current densities. The scan rate was 1 mV/s in All the experiments.

3. Results and discussion

Steady-state voltammetric curves obtained at the Pt electrode are presented in **Figures 2** and **3**. It can be seen that the cathodic limiting reaction (hydrogen evolution reaction) takes place at -0.6 V vs. the Ag/Ag^+ reference electrode and the anodic limiting reaction (oxygen evolution reaction) proceeds at approximately 0.6 V vs. the Ag/Ag^+ reference electrode (**Figure 3**). It can be seen from **Figure 3** that the electrochemical stability window on Pt in the molten $\text{KH}_2\text{PO}_4/\text{K}_2\text{H}_2\text{P}_2\text{O}_7$ at 260°C is approximately 1.67 V .

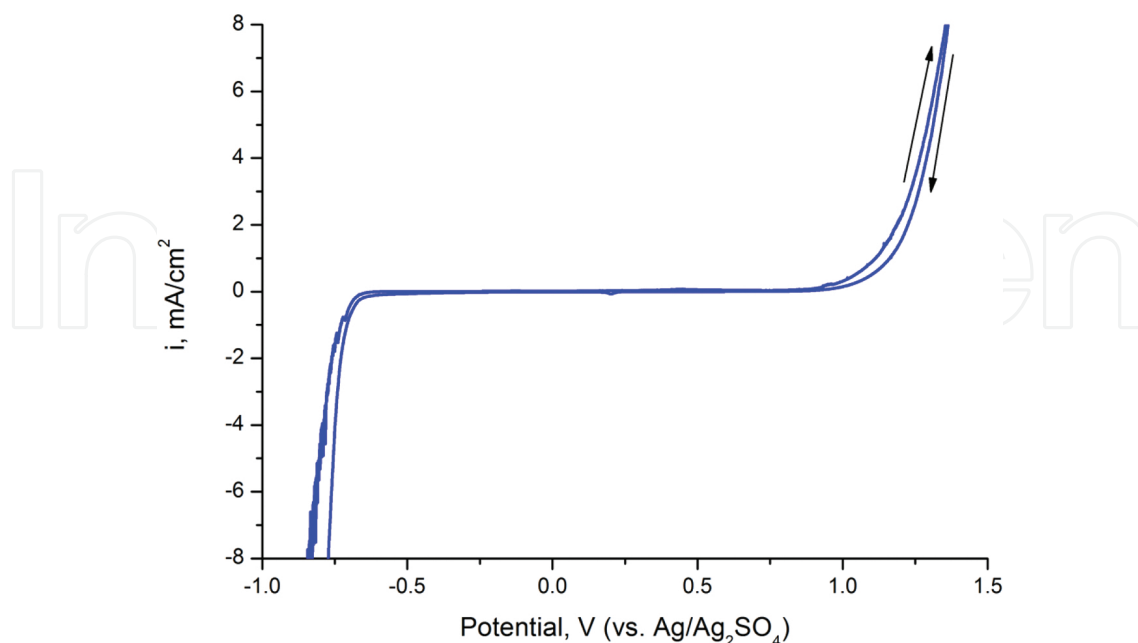


Figure 2. Polarization curve for Pt wire in molten $\text{KH}_2\text{PO}_4/\text{K}_2\text{H}_2\text{P}_2\text{O}_7$ at 260°C . Scan rate 1 mV/s .

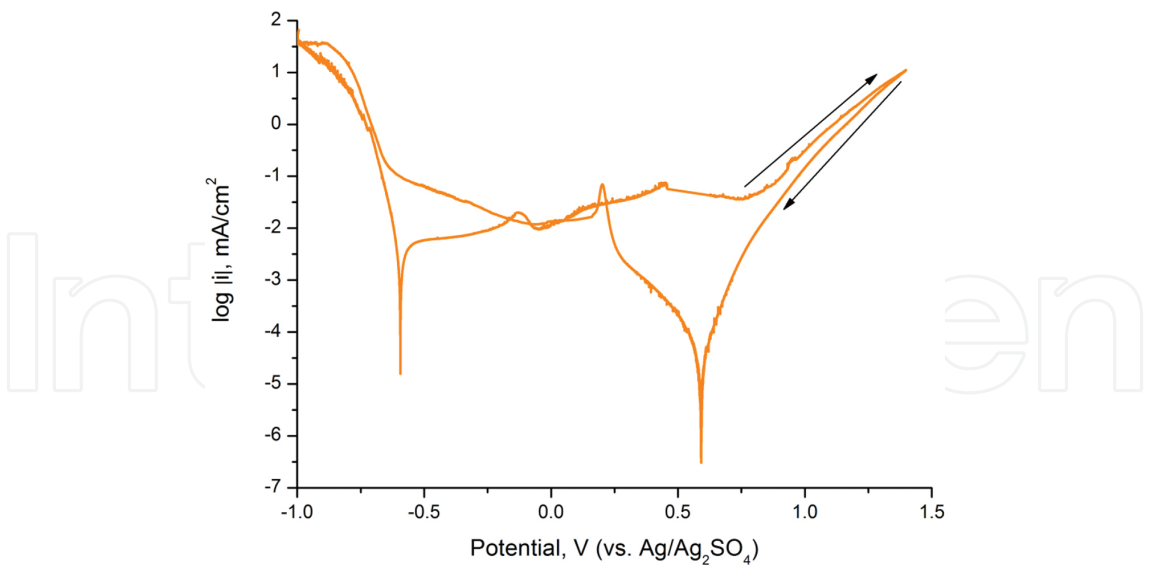


Figure 3. Tafel plot for Pt wire in molten $\text{KH}_2\text{PO}_4/\text{K}_2\text{H}_2\text{P}_2\text{O}_7$ at 260°C . Scan rate 1 mV/s.

It is safe to assume the following limiting reactions:

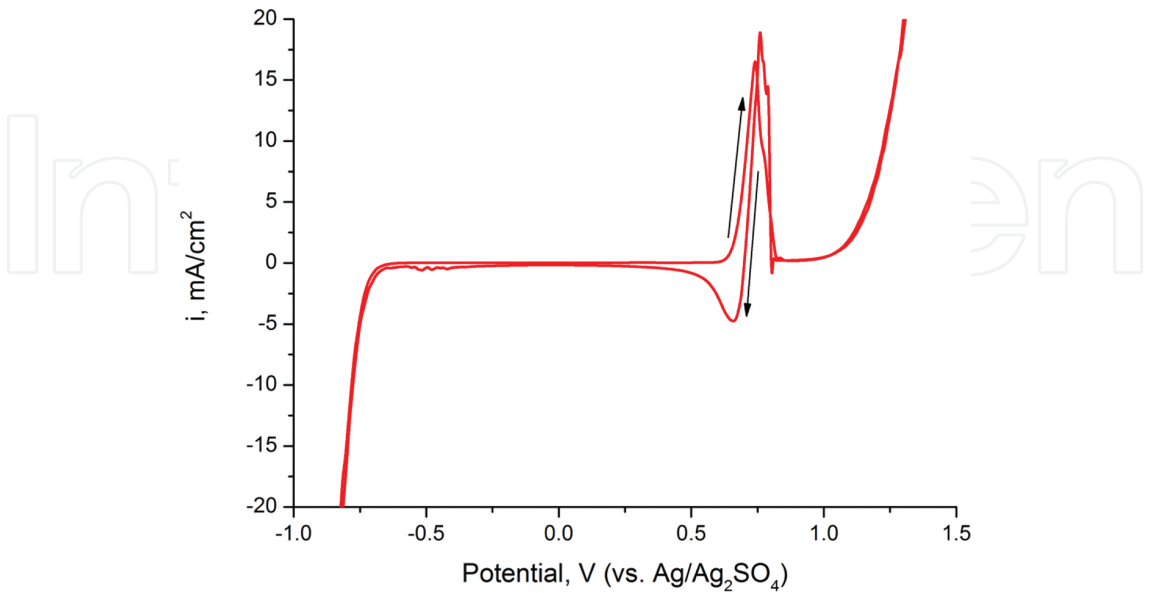


Figure 4. Polarization curve for Au wire in molten $\text{KH}_2\text{PO}_4/\text{K}_2\text{H}_2\text{P}_2\text{O}_7$ at 260°C . Scan rate 1 mV/s.

Moreover, in our recent study [5], electrolysis was performed by passing current through closed ampoules (vacuum sealed quartz glass electrolysis cells with platinum electrodes). The formation of mixtures of hydrogen and oxygen gases as well as water vapor was detected by Raman spectroscopy. In this way, it was demonstrated that water presents in this new type of electrolyte can be electrolyzed at temperatures ~275 to 325°C via the reaction:



The steady-state voltammetric curve obtained at the Au electrode is presented in **Figure 4**. It can be seen that the hydrogen evolution reaction takes place almost at the same potential as at the Pt electrode.

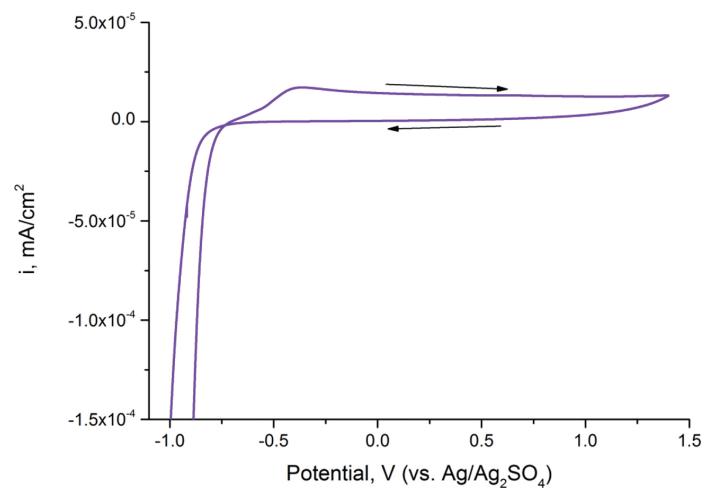


Figure 5. Polarization curve for Ta-CVD coating on AISI 316L wire in molten $\text{KH}_2\text{PO}_4/\text{K}_2\text{H}_2\text{P}_2\text{O}_7$ at 260°C. Scan rate 1 mV/s.

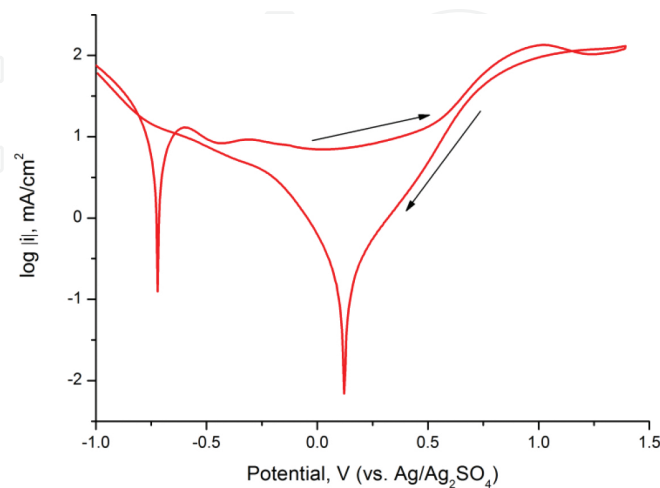


Figure 6. Polarization curve for stainless steel AISI 316L wire in molten $\text{KH}_2\text{PO}_4/\text{K}_2\text{H}_2\text{P}_2\text{O}_7$ at 260°C. Scan rate 1 mV/s.

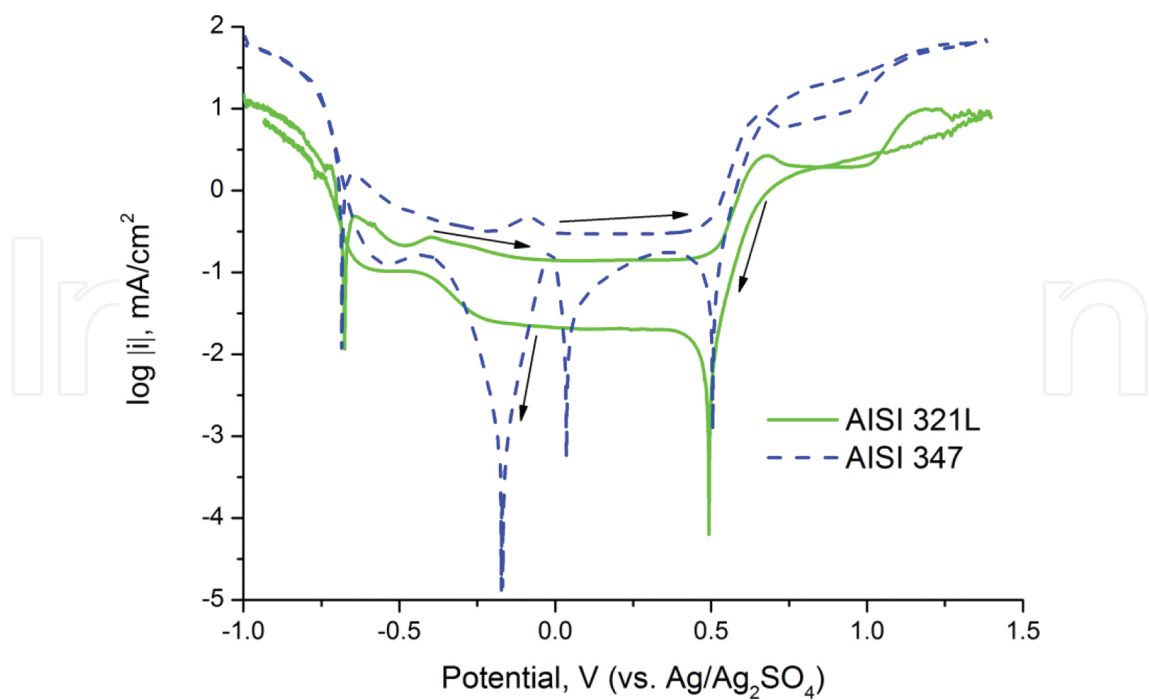


Figure 7. Polarization curves for AISI 321L and AISI 347 wires in molten $\text{KH}_2\text{PO}_4/\text{K}_2\text{H}_2\text{P}_2\text{O}_7$ at 260°C. Scan rate 1 mV/s.

However, like in the molten KHSO_4 , gold demonstrated corrosion instability at positive polarization [12]. There is a reduction-oxidation reaction at around 0.6 V, which can be assumed to be Au electrochemical oxidation and the Au complex reduction, that is, corrosion of gold in molten $\text{KH}_2\text{PO}_4/\text{K}_2\text{H}_2\text{P}_2\text{O}_7$.

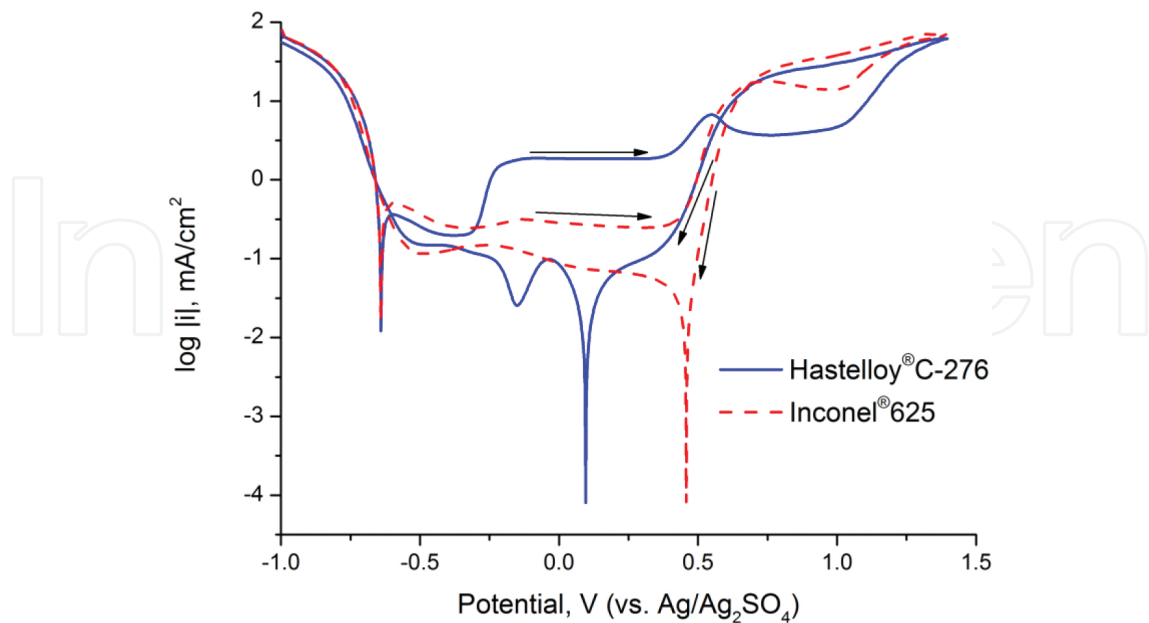


Figure 8. Polarization curves for Hastelloy®C-276 and Inconel®625 wires in molten $\text{KH}_2\text{PO}_4/\text{K}_2\text{H}_2\text{P}_2\text{O}_7$ at 260°C. Scan rate 1 mV/s.

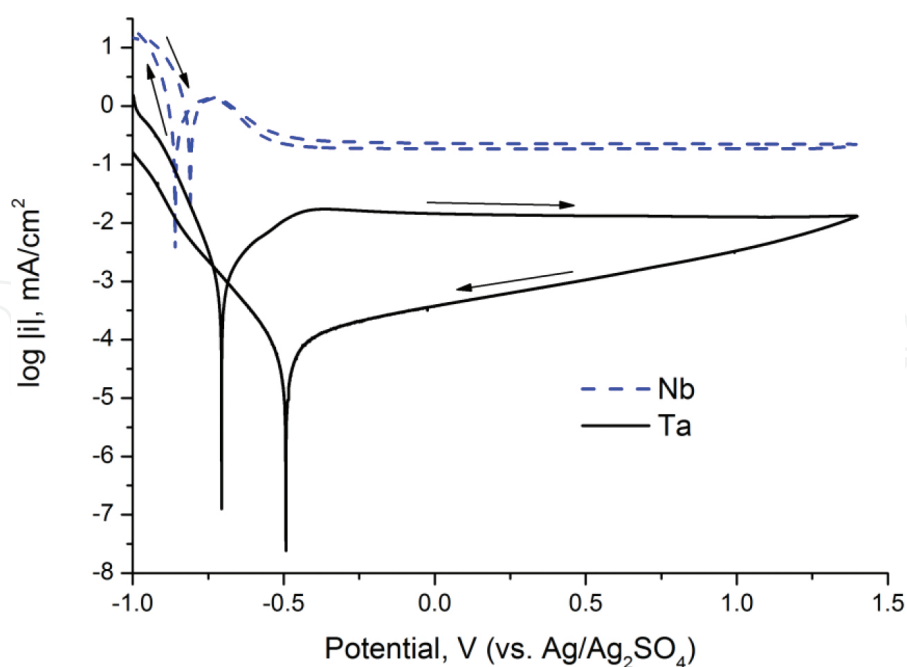


Figure 9. Polarization curves for Nb and Ta wires in molten $\text{KH}_2\text{PO}_4/\text{K}_2\text{H}_2\text{P}_2\text{O}_7$ at 260°C . Scan rate 1 mV/s .

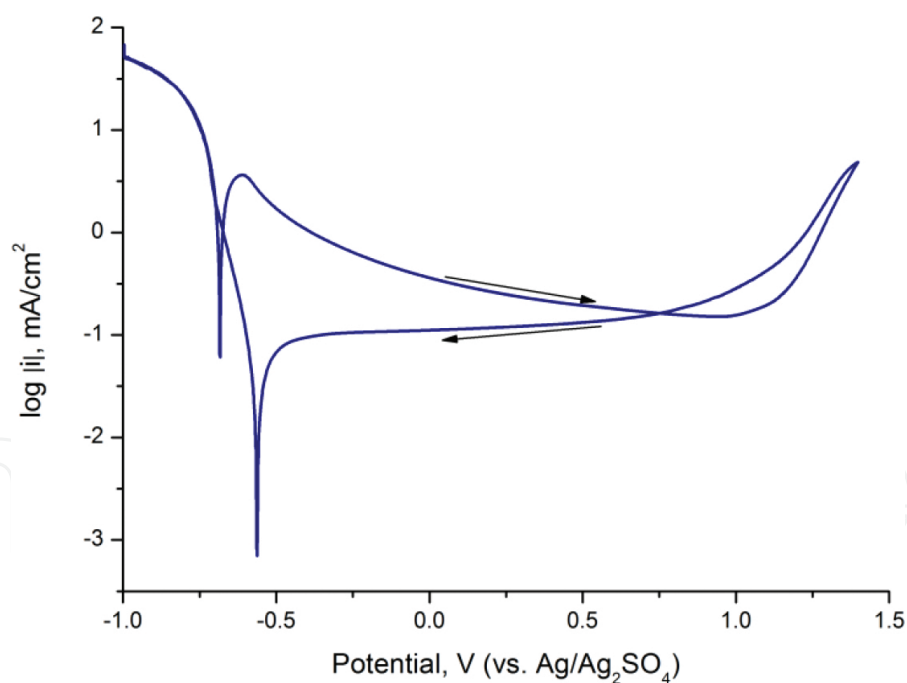


Figure 10. Polarization curve for Ni wire in molten $\text{KH}_2\text{PO}_4/\text{K}_2\text{H}_2\text{P}_2\text{O}_7$ at 260°C . Scan rate 1 mV/s .

The voltammetric data obtained for the stainless steels and the high-nickel alloys are presented in **Figures 5–11** and **Tables 2** and **3**. It can be seen that stainless steels AISI 316 and AISI 347 are corrosion unstable in the studied media (**Figures 6** and **7**), with the AISI 316 undergoing corrosion dissolution at around 0.122 V and the AISI 347 anodically dissolving at -0.04 and

-0.20 V. It is obvious from **Figure 8** that Inconel®625 is more corrosion stable than Hastelloy®C-276. Among the alloys, the behavior is explained by the presence of Ti in the materials. Nb and Ta doping were not effective in preventing corrosion in the alloys. In this study, we did not concentrate on studying particular mechanisms of corrosion in different alloys rather the purpose of this study was to make a review and a selection of materials, which have the potential to be used in this electrolyte.

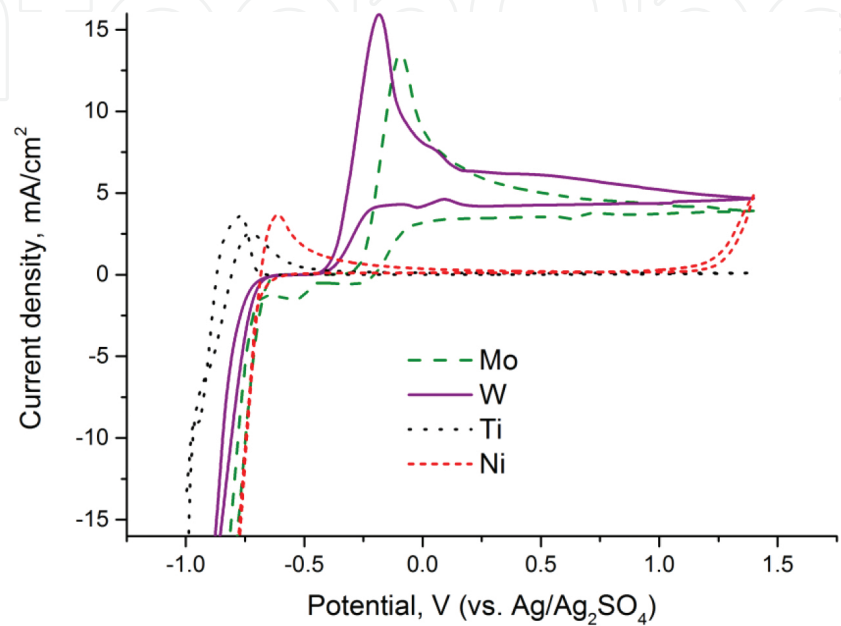


Figure 11. Polarization curves for Ni, W, Ti, and Ni wires in molten $\text{KH}_2\text{PO}_4/\text{K}_2\text{H}_2\text{P}_2\text{O}_7$ at 260°C. Scan rate 1 mV/s.

Sample	Potential vs. $\text{Ag}/\text{Ag}_2\text{SO}_4$ [mV]	
	HER (at forward scan)	OER (at backward scan)
SS AISI 316L	-720	-
SS AISI 321	-675	493
SS AISI 347	-685	505
Hastelloy®C-276	-640	-
Inconel®625	-640	457
Pt	-594	594
Au	-597	699
Tantalum	-705	-
Niobium	-810	-
Nickel	-683	-

Table 2. Reversible potentials, calculated from Tafel curves.

It is also clear from **Figure 9** that at the Ta electrode, the hydrogen evolution reaction (HER) takes place at less negative potentials than at the Nb electrode. However, the HER exchange current is much higher at the niobium electrode. Both metals are electrochemically inactive at positive polarization and have high enough corrosion stability.

Sample	E_{corr} [mV]	i_{corr} [mA/cm ² (CR, mm/year)]
SS AISI 316L	122	1.2×10^{-1} (1.4)
SS AISI 347	36	5.0×10^{-2} (0.6)
Hastelloy®C-276	96	3.0×10^{-2} (0.4)

Table 3. Calculated corrosion currents and corrosion rates (from the backward polarization slope).

Both Ta (**Figure 9**) and Ni (**Figure 10**) demonstrate an obvious passivation at positive polarization (hysteresis between scans in the cathodic and anodic directions).

Comparison between the electrochemical behaviors is shown in **Figure 11**. As it has already been mentioned, Ti and Ni demonstrate high corrosion resistance. This fact is in contrast to earlier results which demonstrated poor stability of titanium in hot phosphoric acid [6]. This can be explained by different acidities of two electrolytes: H_3PO_4 and $\text{KH}_2\text{PO}_4/\text{K}_2\text{H}_2\text{P}_2\text{O}_7$. In contrast to Ti and Ni, there is obvious anodic dissolution with passivation in case of Mo and W between -0.5 and 0.0 V. It should be also mentioned that at Mo, W, and Ni HER takes place at a potential close to the HER potential for Pt. Only at the Ti electrode HER proceeds at more negative potentials.

4. Conclusions

Among the studied materials Pt, Ni, Ta, Ti, AISI 321, and Inconel®625 were the most corrosion stable in the molten $\text{KH}_2\text{PO}_4/\text{K}_2\text{H}_2\text{P}_2\text{O}_7$ at 260° . If we compare the corrosion resistance of the stainless steels and their composition (**Table 1**), we can conclude that Ti as an additive, and not Nb or Ta, increase corrosion resistance of the stainless steels in the studied media. Corrosion resistance of the high-nickel alloys shows that the higher the nickel content and the lower the Mo content the higher is the corrosion resistance.

Author details

Aleksey V. Nikiforov*, Irina M. Petrushina and Niels J. Bjerrum

*Address all correspondence to: nava@dtu.dk

DTU Energy, Technical University of Denmark, Kemitorvet, Denmark

References

- [1] S. Meyer, A. Nikiforov, I. Petrushina, K. Köhler, E. Christensen, J. Jensen, N. Bjerrum, *International Journal of Hydrogen Energy*, 40 (7), 2905 (2015).
- [2] A.V. Nikiforov, I.M. Petrushina, E. Christensen, A.L. Tomas-Garcia, N.J. Bjerrum, *International Journal of Hydrogen Energy*, 36, 111 (2011).
- [3] A.V. Nikiforov, A.L. Tomas Garcia, I.M. Petrushina, E. Christensen, N.J. Bjerrum, *International Journal of Hydrogen Energy*, 36, 5797 (2011).
- [4] J. Polonsky, I.M. Petrushina, E. Christensen, K. Bouzek, C.B. Prag, J.E.T. Andersen, N.J. Bjerrum, *International Journal of Hydrogen Energy*, 37, 2173 (2012).
- [5] R. Berg, A. Nikiforov, I. Petrushina, N. Bjerrum, *Applied Energy*, 2016, submitted.
- [6] O. Ulleberg, T. Nakken, A. Ete, *International Journal of Hydrogen Energy*, 35, 1841 (2010).
- [7] P. Millet, N. Mbemba, S.A. Grigoriev, V.N. Fateev, A. Aukauloo, C. Etiévant, *International Journal of Hydrogen Energy*, 36, 4134 (2011).
- [8] A. Hermann, T. Chaudhuri, P. Spagnol, *International Journal of Hydrogen Energy*, 30, 1297 (2005).
- [9] D. Labou, E. Slavcheva, U. Schnakenberg, S. Neophytides, *Journal of Power Sources*, 185, 1073 (2008).
- [10] Q. Li, J.O. Jensen, R.F. Savinell, N.J. Bjerrum, *Progress in Polymer Science*, 34, 449–477 (2009).
- [11] T. Uda, S.M. Haile, *Electrochemical and Solid-State Letters*, 8, A245 (2005).
- [12] I.M. Petrushina, N.J. Bjerrum, R.W. Berg, F. Cappel, *Journal of the Electrochemical Society*, 144, 532 (1997).
- [13] N.J. Bjerrum, I.M. Petrushina, R.W. Berg, *Journal of the Electrochemical Society*, 142, 1806 (1995).
- [14] L Meites, ed., *Handbook of Analytical Chemistry*, McGraw Hill, NY (1963). Section 5.